

THERMAL INFRARED STUDIES OF SALT CEMENTS; IMPLICATIONS FOR MARS. A. M. Baldridge¹ and P.R. Christensen², ¹Arizona State University, School of Earth and Space Exploration, MC 6305, Tempe, AZ, 85287, alice.baldridge@asu.edu

Introduction: If significant water endured on the surface of Mars, large salt deposits would be expected to form as the water evaporated. Mineralogical and morphological results from the Mars Exploration Rovers (MER) indicate that liquid water did once persist at the surface [1]. Additionally, the Mars Odyssey Gamma Ray Spectrometer (GRS) suggests that water or at least hydrated minerals are present near the Martian surface [2]. On Earth, even in arid environments, salt crusts form at or near the surface indicating the precipitation of minerals in the presence of water [3]. If salt minerals are present and persist in the Martian dust, diurnal condensation and melting of frost could dissolve and concentrate more soluble salts (e.g. halite) at the surface. Crusted surfaces, or duricrusts, have been observed on Mars at both Viking [4-6], Pathfinder [7, 8] and Mars Exploration Rover landing sites and have been inferred from orbital thermal inertia and albedo measurements [9-11].

Chemical analysis at the Martian landing sites indicates elevated levels of sulfur and chlorine in the more cohesive surface materials, which supports the presence of salt crusts. At the Viking landing sites, sulfates are limited to 8-15 wt% [4, 5], ~5wt% at the Pathfinder site [12] and up to 30% at the MER Opportunity landing site based on results from the Miniature Thermal Emission Spectrometer (MINITES). The Mars Reconnaissance Orbiter (MRO) Compact Reconnaissance Imaging Spectrometer for Mars (CRISM) and Mars Express Observatoire pour la Minéralogie, l'Eau, les Glaces, et l'Activité (OMEGA) have identified both Mg- and Ca- sulfates at several locations on Mars although have not reported abundances [13, 14]. Bassanite, gypsum, kieserite, as well as polyhydrated forms of Mg-sulfate have been identified although Fe²⁺ and Fe³⁺ - sulfates have been suggested.

Chlorides on Mars are thought to be associated with sodium in halite, magnesium in bischofite or chloromagnesite and/or calcium in antarcticite. Chloride abundance is limited to minor abundances (~1wt%) at the Viking and Pathfinder and MER landing sites. The GRS mapped chlorine abundance from orbit, although CRISM, OMEGA, TES nor THEMIS have detected chloride salts. Despite these detections, the Thermal Emission Spectrometer (TES) orbiting Mars on the Mars Global Surveyor has not observed mineralogical evidence for salts on the planet's surface [10, 15, 16].

The ability to identify salt deposits on the surface of Mars has significant implications for the role water has played in the planet's past and how water currently interacts with surface materials. Spectroscopy provides a method for detecting salt minerals on Mars

from orbit. This study utilizes thermal infrared laboratory measurements of chloride salt mixtures and crusts to characterize their spectral features to allow for their detection on the Martian surface.

Methods: Thermal infrared spectra of mixtures were measured using the Nicolet Nexus 670 E.S.P FTIR interferometer at Arizona State University's Mars Space Flight Facility (MSFF). Particulate mixtures of chloride salts, specifically halite and MgCl₂*nH₂O were weighed and prepared in Krylon black copper cups. We chose laboratorite as the substrate because of its general similarity to the Martian surface spectra, purity, and availability in quantities necessary for this study. Sample particulates were sieved to <100µm and mixed carefully to ensure homogeneity and poured into sample cups. Samples were heated for several hours at 80C to eliminate adsorbed water. Following the measurement of particulates the samples were sprayed with a fine mist of distilled H₂O, dried for several more hours at 80C and measured again. The fine mist dissolves salt at the surface of the sample and as the water evaporates in the oven, a delicate crust forms at the sample surface. Additionally particulate mixtures were pressed into 1 cm diameter pellets with a hydraulic press. This approximates a specular surface resulting in a high contrast spectral signal [17]. The pellets also approximate an indurated crust, filling pore spaces without concentrating salt at the sample surface due to evaporative pumping. Thus, the weight percent of halite and substrate is preserved at the surface.

Results:

Halite. The detection of halite in infrared spectra is challenging because it is transparent over much of the infrared region of the electromagnetic spectrum. Halite itself is often described as spectrally featureless in the IR and its detection must be based on the effect it has on the spectra of surrounding materials. For example, due to transparency, even small amounts of contaminants, such as trace sulfate and minor adsorbed water, can have pronounced spectral features [18-21]. The spectrum of <100µm loose particulates of reagent grade halite is shown in Figure 1. The absorption of halite in this region of the spectrum is at 264cm⁻¹. The features at ~1600cm⁻¹ and ~1200cm⁻¹ are transparency features associated with water and sulfate respectively. The low broad emissivity of halite at high wavenumbers is characteristic of most halite samples. Only when the sample has significant contamination does the emissivity in this region increase. Additionally, *Eastes* [19] showed that in the presence of halite,

spectra of particulate minerals were inverted, shifted to shorter wavelengths and the spectral contrast increased near absorption bands. *Eastes* [19] described this behavior as ‘transmission-like’ and similar to volume scattering effects induced by decreased particle size [22-25]. In samples of halite crusts collected from Badwater Basin, Death Valley, the ‘transmission-like’ features were significantly pronounced, having a spectral contrast of 30% (as opposed to 10% in samples with halite crusts) [21].

Emission spectra of halite and laboritorite mixtures are shown in Figure 2 and 3. Figure 3 zooms in to examine the subtle differences between the mixtures with 5, 10 and 25% halite. With the addition of halite, the spectral features of laboritorite begin to shallow and emissivity is initially increased at high wavenumbers. With the addition of 25% halite, the spectral features of laboritorite begin to invert and emissivity decreases at high wavenumbers. The 50% halite mixture shows a clear inversion of the silicate absorptions and with 75% the low broad emissivity with an upward slope toward low wavenumbers, characteristic of halite, is evident. The spectra of the ‘crusted’ mixtures show a similar effect except that the silicate features shift to lower wavenumbers almost immediately but do not invert until 75% halite abundance. The decrease in emissivity is also not as pronounced as in particulate mixtures (Figure 4).

The emission spectrum of $MgCl_2 \cdot nH_2O$ used for mixtures is shown in Figure 1. Previous IR studies of $MgCl_2$ are limited, describing only the position of absorptions associated hydration [26]. Two spectra of $MgCl_2 \cdot nH_2O$ are given here in Figure 6 ($MgCl_2 \cdot nH_2O$ A and B). $MgCl_2 \cdot nH_2OA$ is $<100\mu m$ particulates that have been baked in the oven at 80C for several days to remove water. Despite this, the sample spectrum still shows a pronounced water feature at $1600cm^{-1}$. This could be due to the transparency of $MgCl_2$ in this region of the spectrum, similar to halite, or due to scattering by clinging fines on the small dehydrated crystals as seen with the dehydration of gypsum crystals [17]. $MgCl_2 \cdot nH_2OB$ is granular, crystalline, reagent grade $MgCl_2$. This spectrum is featureless over the entire spectral region. Both spectra have a positive slope with a maximum emissivity of ~ 0.95 .

Emission spectra of $MgCl_2 \cdot nH_2O$ and laboritorite mixtures are shown in Figure 5. The addition of $MgCl_2 \cdot nH_2O$ decreases silicate spectral contrast. The water feature is evident with only 5% $MgCl_2 \cdot nH_2O$. With the addition of more than 25% chloride the transparency features associated with $MgCl_2 \cdot nH_2O$ become pronounced including the slope toward high wavenumbers. XRD of the $MgCl_2 \cdot nH_2O$ will be measured to confirm mineralogy. Additional work will measure the spectra of crusts formed with these mixtures as well as pressed pellets to simulate indurated surfaces.

Discussion: Emission spectra of the chlorides measured are given in Figure 6 including sylvite (KCl),

halite and $MgCl_2 \cdot nH_2O$. Additional measurements will include Ca- and Fe-chlorides. The halite spectra A and B are from [20] and represent a natural halite sample from Searle’s Lake and a hand sample from Detroit. Kinetic sample temperature experiments in this study show that halite has an emissivity very close to 1 at high wavenumbers and therefore is not a greybody in this region. However, Halite A is unique from all other halite samples measured in that it is spectrally featureless with a high overall emissivity and may exhibit greybody properties due to contaminants. Similarly, two very different Mg-chloride spectra are shown; one with transparency features ($MgCl_2 \cdot nH_2OA$) and one that appears spectrally featureless ($MgCl_2 \cdot nH_2OB$). The reason for these differences is not yet well understood, but is probably related to the isometric properties of chloride minerals. Future work will examine the sample contaminants in addition to the determining the maximum emissivities of chlorides.

[27] and [28] have identified a spectrally unique unit several regions on Mars that they have termed ‘glowing terrain’. These regions are such named because they glow blue and stand out in Thermal Emission Imaging System (THEMIS) decorrelation stretch images indicating that the data have a maximum value at low wavelength ($\sim 8.5\mu m$) decreasing in emissivity with increasing wavelength. Additionally, TES data over these regions show an overall decrease in emissivity over the entire wavelength range. The presence of a material that acts as a greybody such as a chloride salt is suggested to cause this slope. Recent HRSC images of these regions suggest that the surface is indeed cemented by a light colored material [29]. Gamma Ray Spectrometer (GRS) chlorine maps agree with the presence of a chloride mineral at $\sim 0.8\%$ in some of the glowing terrain regions [30].

Terrestrial playa lakes are considered important potential analogs for paleolake basins proposed for Mars. Playas are typically zoned mineralogically, based on the relative solubility of salts [31, 32] and, if unmodified from the time of deposition (i.e. impacts, aeolian deflation and deposition), the pattern of resulting evaporites should be detectable with remote sensing. Typical evaporite assemblages predicted for Mars assume a mafic parent rock and include carbonates, sulfates, phosphates and chlorides. If the glowing terrain does represent halite-cemented sediments, sulfates might be expected to be present as well based on evaporation sequences. However, sulfates have not been detected in these regions in either the thermal infrared with TES, nor the VIS Near-IR with OMEGA or CRISM. Moreover, salt cements are expected to have been broken down and reworked by aeolian deflation since time of deposition and may be present globally in dust. Additionally, if water is interacting with the surface as the deposition, melting and evaporation of frost, this amount of water may be enough to

dissolve only the most soluble salts like halite. All chloride salts of the four candidate major cations (Na, Mg, Ca, Fe) are quite soluble. Therefore, unless these deposits represent original evaporative sequences from abundance surface water, sulfates may not be present.

The GRS measurements indicate an abundance of ~1% chloride at some of these regions on Mars measured the upper tens of centimeters, while TES and THEMIS are measuring the upper few microns. Therefore evaporative pumping could easily concentrate the salt at the surface in abundances well above a facilitating their detection in the IR.

The calibration techniques used for the TES and Mini-TES instruments, in addition to laboratory thermal infrared spectrometer at ASU, make the assumption that over some portion of the spectrum the emissivity is equal to 1 (reflection equaling zero). This is most closely met at the Christiansen frequency where minerals display an emissivity maximum related to the optical constants n and k . Making this assumption allows the sample radiance variable to be isolated in order to determine sample temperature. This assumption works well for most natural materials, which have emissivity maximum close to one. For materials that behave as a greybody however, such as $MgCl_2 \cdot nH_2O$ as reported above, this assumption does not hold. By "fixing" the emissivity to 1, a brightness temperature lower than the kinetic temperature of the sample is used in determining sample emissivity, which induces a slope toward low wavenumbers. For $MgCl_2 \cdot nH_2O$ the effect of this slope is actually to flatten out the spectrum.

Conclusions: While neither the Na- or Mg- chloride measured here support a negative slope as seen by TES for the glowing terrain, other chloride samples may be responsible for this effect. For example Halite A does appear to have a slight negative slope. The mixtures and cements of chlorides do have diagnostic features, however, that will aid in their remote detection. Namely, both Mg and Na chlorides have transparency features at high wavenumbers and thus induce positive slopes in the data.

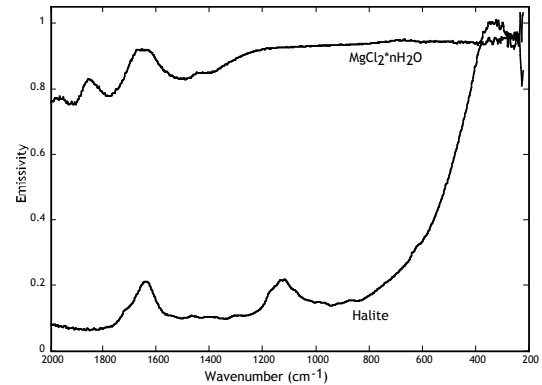


Figure 1. Thermal emission spectra of NaCl (halite) and $MgCl_2 \cdot nH_2O$ used for mixtures in this study.

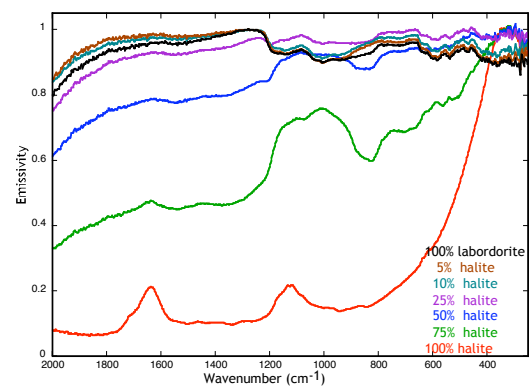


Figure 2. Thermal emission spectra of particulate mixtures of halite and laboritorite.

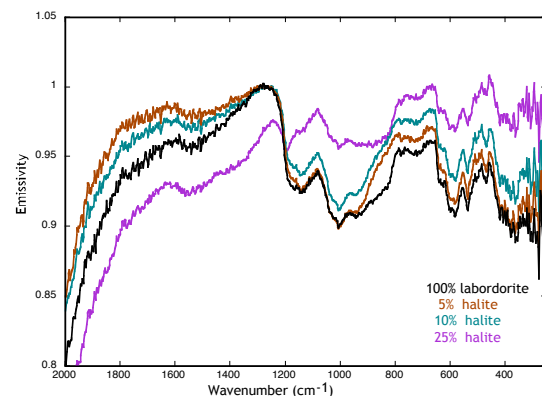


Figure 3. Thermal emission spectra of particulate mixtures of halite and laboritorite, scaled to examine subtle changes between 5, 10 and 25% halite.

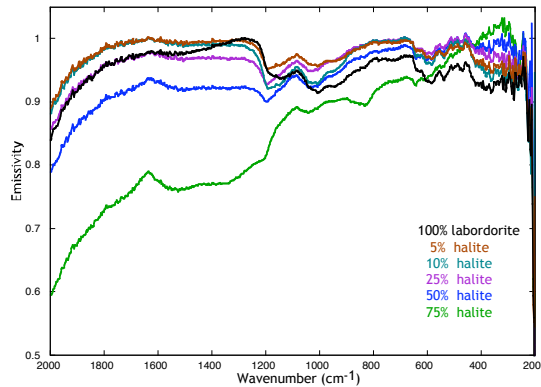


Figure 4. Thermal emission spectra of halite and labor-dorite crusts.

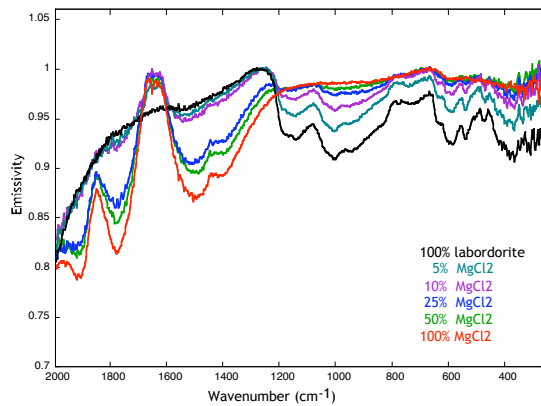


Figure 5. Thermal emission spectra of particulate mixtures of $MgCl_2 \cdot nH_2O$ and labordorite.

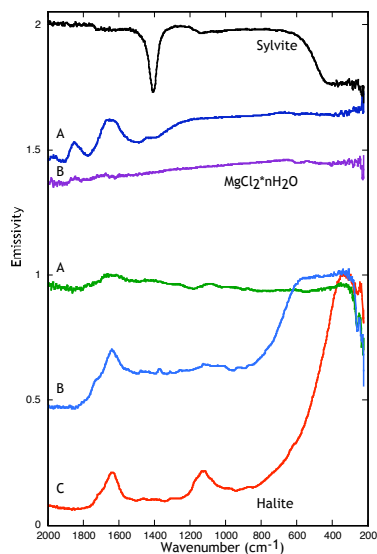


Figure 6. Thermal emission spectra of chloride minerals.

References: [1] Squyres, S.W., et al. (2004) *Science*, 306(1709-1714). [2] Boynton, W.V., et al. (2002) *Science*, 297(5578), 81-85. [3] (1997), *Arid zone geomorphology : process, form, and change in drylands*. [4] Clark, B.C., et al. (1976) *Science*, 194(4271), 1283-1288. [5] Clark, B.C. and D.C. Van Hart (1981) *Icarus*, 45(2), 370-378. [6] Baird, A.K., et al. (1976) *Science*, 194(4271), 1288-1293. [7] Rieder, R., et al. (1997) *Science*, 278(5344), 1771-1774. [8] Matijevic, J.R., et al. (1997) *Science*, 278(5344), 1765-1768. [9] Bandfield, J.L. and M.D. Smith (2003) *Icarus*, 161(1), 47-65. [10] Christensen, P.R., et al. (2001) *JGR*, 106(E10), 23823-23871. [11] Jakosky, B.M. and P.R. Christensen (1986) *JGR*, 91(B3), 3547-3559. [12] Bell, J.F., III, et al., *Mineralogic and compositional properties of Martian soil and dust; results from Mars Pathfinder, in Results from Mars Pathfinder, Part 2.*, P. Golombek Matthew, Editor. 2000, American Geophysical Union. Washington, DC, United States. 2000. [13] Gendrin, A., et al. (2005) *Science*, 307(1587-1591). [14] Murchie, S., et al. (2006) *AGU Fall Meeting Abstracts*, 3304. [15] Bandfield, J.L. (2002) *JGR*, 107(E6), art. no.-5042. [16] Christensen, P.R., et al. (2000) *JGR*, 105(E4), 9623-9642. [17] Baldrige, A.M. and P.R. Christensen (2007) *Lunar and Planetary Institute Conference Abstracts*, 2407. [18] Crowley, J.K. and S.J. Hook (1996) *JGR*, 101(B1), 643-660. [19] Eastes, J.W. (1989) *Remote Sens Environ*, 27(3), 289-303. [20] Lane, M.D. and P.R. Christensen (1998) *Icarus*, 135(2), 528-536. [21] Baldrige, A.M., et al. (2004) *JGR*, 109(12006). [22] Salisbury, J.W. and A. Wald (1992) *Icarus*, 96(1), 121-128. [23] Salisbury, J.W. and J.W. Eastes (1985) *Icarus*, 64(3), 586-588. [24] Vincent, R.K. and G.R. Hunt (1968) *Appl Optics*, 7(1), 53-&. [25] Hunt, G.R. and R.K. Vincent (1968) *JGR*, 73(18), 6039-&. [26] Gurevich, L.M., et al. (1977) *J Struct Chem+*, 18(5), 683-687. [27] Glotch, T.D., et al. (2007) *Lunar and Planetary Institute Conference Abstracts*, 1820. [28] Osterloo, M.M., et al. (2007) *Lunar and Planetary Institute Conference Abstracts*, 1814. [29] Osterloo, M. 2007. [30] Keller, J.M., et al. (2006) *JGR*, 111(E3), -. [31] Hunt, C.B., *The Death Valley salt pan, a study of evaporites*. 1960, U.S. Geological Survey: Reston, VA. p. B456-B458. [32] Eugster, H.P. and L.A. Hardie, *Saline lakes, in Lakes; chemistry, geology, physics.*, A. Lerman, Editor. 1978, Springer-Verlag: New York, N.Y., United States. p. 237-293.

Acknowledgements: We would like to thank M. Osterloo and T. Glotch for inclusion in discussions of the “glowing terrain”. It is also necessary to acknowledge J.L. Bandfield for many hours of extremely useful and appreciated discussions regarding spectroscopy and help sorting out thoughts as to the nature of salts in the IR.